

# Elucidating the initial dynamics of electron photodetachment from atoms in liquids using variably-time-delayed resonant multiphoton ionization

Ignacio B. Martini and Benjamin J. Schwartz<sup>a)</sup>

*Department of Chemistry and Biochemistry, University of California—Los Angeles, Los Angeles, California 90095-1569*

(Received 20 November 2003; accepted 9 April 2004)

We study the photodetachment of electrons from sodium anions in room temperature liquid tetrahydrofuran (THF) using a new type of three-pulse pump–probe spectroscopy. Our experiments use two variably-time-delayed pulses for excitation in what is essentially a resonant 1+1 two-photon ionization: By varying the arrival time of the second excitation pulse, we can directly observe how solvent motions stabilize and trap the excited electron prior to electron detachment. Moreover, by varying the arrival times of the ionization (excitation) and probe pulses, we also can determine the fate of the photoionized electrons and the distance they are ejected from their parent Na atoms. We find that as solvent reorganization proceeds, the second excitation pulse becomes less effective at achieving photoionization, and that the solvent motions that stabilize the excited electron following the first excitation pulse occur over a time of  $\sim 450$  fs. We also find that there is no spectroscopic evidence for significant solvent relaxation after detachment of the electron is complete. In combination with the results of previous experiments and molecular dynamics simulations, the data provide new insight into the role of the solvent in solution-phase electron detachment and charge-transfer-to-solvent reactions. © 2004 American Institute of Physics. [DOI: 10.1063/1.1756874]

## I. INTRODUCTION

Multiple-pulse femtosecond spectroscopies offer a powerful new method for studying the dynamics of atomic and molecular species.<sup>1–6</sup> Most forms of such spectroscopies rely on investigating the properties of molecules in an electronic<sup>1,2</sup> or vibrational<sup>3,4</sup> coherence, providing information that can be used to deconvolve the effects of system–bath interactions on chromophores embedded in condensed phases. In this paper, we show how even in the absence of coherence, multiple-pulse spectroscopies that explore electronic population dynamics also can provide useful information about system–bath coupling. In particular, we make use of a three-pulse pump–probe sequence to map out the initial dynamics and the nature of the bath relaxation following photoexcitation and detachment of an electron from an atom dissolved in a room temperature liquid. The experiment we perform is essentially a 1+1 two-photon resonant atomic ionization: Information on the role of the liquid in the photoionization process is obtained by measuring the effectiveness of the second pulse in ionizing the atom as a function of the delay time after the first pulse.

The ionization process that we have chosen to study is the photodetachment of an electron from a sodium anion ( $\text{Na}^-$ , or sodide) in room temperature liquid tetrahydrofuran (THF).<sup>7–11</sup> The photon energies we employ in our experiment are below threshold, so that the photoionization of  $\text{Na}^-$  in solution is not direct. Instead, electron detachment is delayed because it cannot occur until after rearrangement of the

local solvent environment.<sup>12</sup> This type of solvent-assisted photodetachment is often referred to as charge-transfer-to-solvent, or CTTS,<sup>13</sup> and has been observed for a variety of molecular and atomic species in solution.<sup>14,15</sup> The absorption spectrum of the  $\text{Na}^-$  CTTS band in THF is shown as the solid curve in Fig. 1(A). This absorption band represents a bound-to-quasi-bound transition, in which excitation of one of the  $\text{Na}^- 3s$  electrons produces an electron bound in the roughly spherical box created by the solvent cavity surrounding the anion.<sup>7</sup> When the solvent molecules move in response to this excitation, the electron can detach (a process that we have measured to take  $\sim 0.7$  ps),<sup>7</sup> creating a solvated electron and a solvated Na atom whose equilibrium absorption spectra are also shown in Fig. 1(A) as the dotted and dashed curves, respectively.

In a series of recent publications, we studied the CTTS dynamics of  $\text{Na}^-$  in THF using conventional two-pulse femtosecond pump–probe spectroscopy and found that electron detachment produces solvated electrons that localize at specific distances from the Na atom, as depicted in Fig. 1(B).<sup>7–9</sup> Upon CTTS excitation, the electron can access one of two possible detachment routes: Low-energy excitation predominantly produces an excited-state wave function that remains well confined in the original solvent cavity with the Na atom, so that the majority of the electrons relax by localizing in the same cavity as their parent sodium anions to form “immediate” contact pairs. The solvated electrons in immediate pairs have significant wave function overlap with their nearby Na atom partners, leading to rapid recombination in  $\sim 1$  ps. In contrast, higher-energy excitation ( $\lambda \approx 400$  nm) promotes electrons to the conduction band of the solvent; upon relax-

<sup>a)</sup>Author to whom correspondence should be addressed. Telephone: (310) 206-4113; Fax: (310) 206-4038. Electronic mail: schwartz@chem.ucla.edu

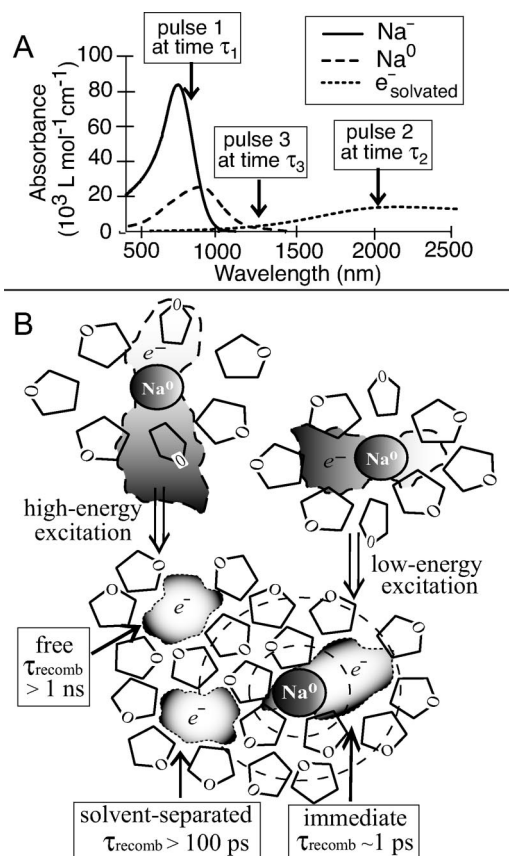


FIG. 1. (A) Absorption spectra of the species involved in the photodetachment of  $\text{Na}^-$  in THF. The arrows show the spectral positions of the laser pulses used in the experiment. (B) Schematic of the  $\text{Na}^-$  photodetachment and recombination reactions. The right side of the figure shows how low-energy excitation produces an excited state contained primarily inside the original solvent cavity that subsequently relaxes by ejection of the electron into an immediate contact-pair that recombines in  $\sim 1$  ps. The left side of the figure depicts how higher-energy excitation generates a spatially larger wave function that relaxes either into solvent-separated contact pairs or free solvated electrons, which recombine in hundreds of ps or do not recombine on sub-ns time scales, respectively.

ation, these highly delocalized electrons can access solvent cavities located more than one solvent shell away from their parent Na atoms, producing “free” solvated electrons that do not recombine on sub-ns time scales. Finally, regardless of the excitation wavelength, we found that a few electrons localize in “solvent-separated” contact pairs, one solvent shell away from their parent Na atoms.<sup>8</sup> Due to negligible wave function overlap, solvent-separated electrons do not recombine for hundreds of ps. Both three-pulse pump-probe experiments<sup>9,10</sup> and mixed quantum/classical molecular dynamics simulations<sup>16</sup> support the general picture of the  $\text{Na}^-$  photodetachment process presented in Fig. 1(B).

In this paper, we present the results of new three-pulse experiments on the  $\text{Na}^-$ -THF system, using time-delayed resonant 1 + 1 two-photon ionization to map out the initial dynamics of the solvent relaxation following CTTS excitation. In these incoherent two-dimensional experiments, we can directly observe the initial solvent motions that lead to CTTS detachment by monitoring how the effectiveness of the second ionization pulse changes as a function of its time delay after the first excitation pulse. We find that the initial

solvent motions take 450 fs to stabilize the CTTS excited state, and that once detachment is complete, essentially no additional solvent relaxation takes place. In combination with the results of previous work on this system from both our group<sup>7–10</sup> and others,<sup>11</sup> the new data allow us to present a refined molecular picture of electron photodetachment in liquids and demonstrate that even incoherent multipulse ultrafast spectroscopies can provide a great deal of insight into condensed-phase reaction dynamics.

## II. EXPERIMENT

In the three-pulse experiments discussed below, the  $\text{Na}^-$ -THF solutions were prepared following a modification of a technique originally described by Dye,<sup>17</sup> our particular implementation of the sample preparation has been presented in detail in a previous publication.<sup>18</sup> The ultrafast spectroscopic experiments were performed with a setup that also has been described in detail elsewhere,<sup>19</sup> other than the time orderings of the pulses, the setup is essentially identical to that presented in our previous three-pulse work.<sup>9,10</sup> In brief, 80% of the 790 nm light of a regeneratively amplified Ti:Sapphire laser ( $\sim 1$  mJ pulses of  $\sim 100$  fs duration at 1 kHz) was used to pump a double-pass optical parametric amplifier (OPA) that produced tunable infrared signal and idler beams. Part of the remaining 20% of the fundamental light, pulse 1 (which arrived at the sample at time  $\tau_1$ ), was used to excite  $\text{Na}^-$  in THF. The  $\sim 2$   $\mu\text{m}$  idler beam from the OPA, pulse 2 (which arrived at time  $\tau_2$ ), served to re-excite the electrons excited by pulse 1. The  $\sim 1250$  nm signal beam from the OPA, pulse 3 (which arrived at time  $\tau_3$ ), served as a probe of the effects of the first two pulses. The spectral positions and time ordering of the three pulses are summarized in Fig. 1(A). In all of the experiments shown below, we choose the arrival time of pulse 1 as the absolute position of the zero of time:  $\tau_1 = 0$ . Pulses 2 and 3 arrived at the sample after a controlled variable time delay by either using a computer-controlled optical delay line or using transparent materials of known index of refraction to vary the optical path length.

The temporal resolution in each of the two time dimensions in our three-pulse experiments was determined by experimentally cross-correlating the 790 nm initial excitation pulse with each of the two time-delayed pulses using sum-frequency generation in a nonlinear optical crystal (BBO). Examples of these cross-correlation functions are presented as the dashed curves in Figs. 3(A) and 3(B), below. As with our previous work,<sup>7,10</sup> for the three-pulse experiments presented below, a Gaussian convolute-and-compare procedure determined the time resolution of our experimental system to be on the order of 200 fs. The time resolution of our apparatus is also verified by the solid curve in Fig. 2(A), below. This 790 nm pump/1250 nm probe two-pulse scan of  $\text{Na}^-$  in THF shows an instrument-limited rise followed by a clearly resolved fast decay component and then a subsequent slower rise. Ruhman and co-workers have measured these same dynamics with  $\sim 50$  fs time resolution, and determined that the fast decay takes place in  $\sim 200$  fs;<sup>11</sup> as this fast decay component is clearly resolved in our data, it is clear our apparatus allows us to confidently measure *all* the dynamics of this system, even the fastest that occur on time scales of  $\sim 200$  fs.

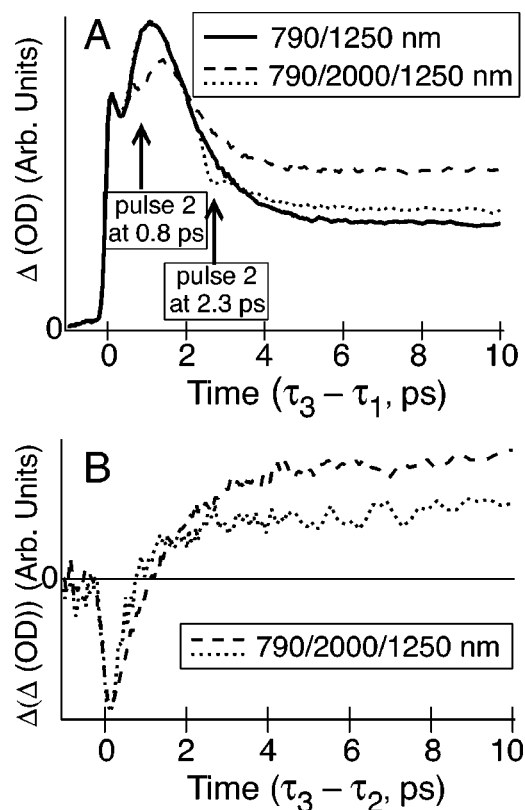


FIG. 2. (A) 2-pulse (solid curve) and three-pulse (dotted and dashed curves) experiments exciting  $\text{Na}^-$  at 790 nm at time zero and scanning the probe pulse at 1250 nm. The arrows indicate the fixed time of re-excitation by the 2000 nm pulse in the three-pulse experiments. (B) Difference signal calculated by subtracting the three- and two-pulse experiments from A (same symbols as the three-pulse experiments in A); for this panel, the arrival of the 2000 nm pulse is chosen as time zero.

### III. RESULTS

#### A. Geminate recombination and delocalization dynamics along the $\tau_3$ time dimension

The solid curve in Fig. 2(A) shows the results of a standard two-pulse transient absorption experiment in which the  $\text{Na}^-$  CTTS band is excited with a 790 nm laser pulse and the photodetachment products are monitored at 1250 nm. The data show an instrument-limited rise that we have attributed to absorption from the excited cavity-confined electron prior to detachment ( $\text{Na}^-*$ ); this absorption then decays rapidly as solvent motions alter both the oscillator strength and the positions of the energy levels involved in this transition.<sup>10</sup> The subsequent  $\sim 1$  ps rise in the signal reflects the appearance of solvated electrons (and solvated Na atoms) due to the ejection process, while the following decay over the next few ps results from the disappearance of immediate-contact-pair electrons due to recombination. The plateau in the data that persists at times longer than  $\sim 6$  ps results from longer-lived solvent-separated and free solvated electrons [cf. Fig. 1(B)].<sup>7,8</sup> We note that an alternative interpretation of the early-time  $\text{Na}^-$  CTTS detachment dynamics following 790 nm excitation has been offered by Ruhman and co-workers.<sup>11</sup> In what follows, however, we will place the experimental results presented below within the context of the picture built

from our previous work [Fig. 1(B)],<sup>7-10</sup> but we will return to consider the alternative view below in the discussion section.

In addition to the two-pulse pump-probe signal, the dashed and dotted curves in Fig. 2(A) show the results of three-pulse experiments.<sup>9,10</sup> In these three-pulse experiments, the first pulse excites  $\text{Na}^-$  in THF at 790 nm, the second pulse, at 2000 nm, re-excites the excited electron at the time indicated by the arrows in the figure, while the third pulse probes the effect of the first two pulses at 1250 nm. Figure 2(B) shows the (normalized and time-shifted) difference between the three-pulse and two-pulse signals, which we will refer to as the “difference signal.” Clearly, the initial effect of the 2000 nm re-excitation pulse is to *decrease* the 1250 nm absorbance of the solvated electrons produced by the 790 nm excitation pulse. This is because the 2000 nm pulse bleaches the ground-state absorption of the solvated electron, which also has significant oscillator strength at 1250 nm [cf. Fig. 1(A)]. The excited solvated electrons have a highly delocalized “conduction-band”-like wave function that extends across a volume much larger than the original solvent cavity. Therefore, as the bleach recovers and the excited solvated electrons relax back to their ground electronic state, they also potentially can *relocalize* into a solvent cavity different from the original one. For example, following re-excitation at 2000 nm, immediate contact pair electrons can be transformed into solvent-separated or free electrons.<sup>9,10</sup> This relocalization of the immediate contact pair electrons can be thought of as a resonant ionization process, or equivalently, as a  $1+1$  resonant ionization of the original sodium anions. Evidence for this transformation of immediate-pair electrons into free solvated electrons is seen in both panels of Fig. 2, where it is clear that application of the 2000 nm pulse both suppresses the fast recombination of immediate contact pairs and increases the magnitude of the 1250 nm absorbance that results from the presence of longer-lived electrons and Na atoms.<sup>9,10</sup>

Although three-pulse experiments of the type shown in Fig. 2 verify the ability of a 2000 nm pulse to relocalize immediate-pair solvated electrons, they provide only limited information because they are one-dimensional: Only the time of the third pulse ( $\tau_3 - \tau_1$ ) is scanned. However, the two experiments shown in Fig. 2 indicate that the time at which the second pulse arrives also has an important effect on relocalization. The difference signals in Fig. 2(B) are normalized to the maximum of the electron bleach, which is proportional to the number of electrons that were re-excited by the 2000 nm pulse. When normalized this way, it is clear that the efficiency of relocalization, measured by the positive “relocalization offset” in the difference signal at long times, depends on the time that the 2000 nm re-excitation pulse arrived relative to the 790 nm excitation pulse: In other words, if the 2000 nm re-excitation pulse arrives *during* the electron detachment process [which we assign to the slower rise component of the solid curve in Fig. 2(A)],<sup>8</sup> a larger number of free electrons are created by re-excitation than if the 2000 nm pulse arrives after detachment is complete. The fact that the ability to perform  $1+1$  resonant photoionization of  $\text{Na}^-$  in solution depends on exactly when the second pulse is applied tells us that the early-time dynamics following the

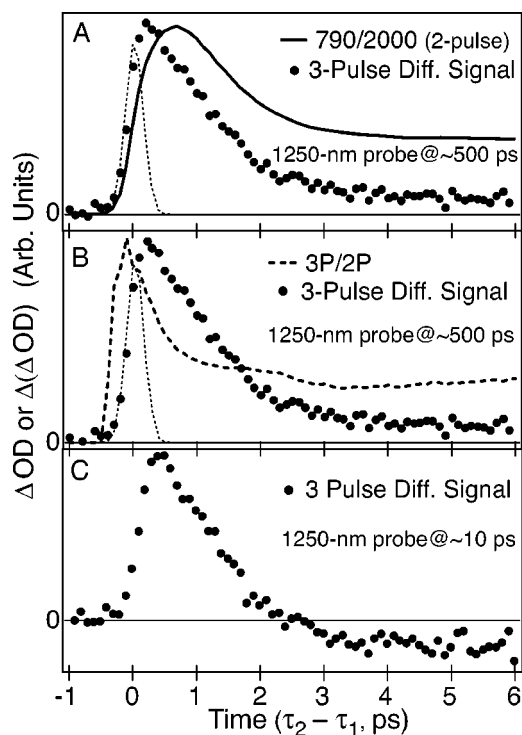


FIG. 3. (A) Comparison of a two-pulse 790 nm pump/2000 nm probe experiment (solid curve) on  $\text{Na}^-$  in THF with the difference signal for an experiment exciting at 790 nm at time zero and scanning the 2000 nm re-excitation pulse while probing with a 1250 nm pulse fixed at 500 ps (circles). (B) Circles are the same signal as panel A, and the dashed curve is the ratio of the three-pulse difference and two-pulse signals from A (3P/2P). (C) 3-pulse difference signal as in A and B, except that the 1250 nm probe pulse is fixed at 10 ps instead of 500 ps (circles). The thin dashed curves around the zero of time in panels (A) and (B) show the cross-correlation (instrument response function) of the 790 and 2000 nm excitation pulses measured via sum frequency generation in a BBO crystal.

initial excitation are complex: The more time that has elapsed since the original excitation, the more the solvent has relaxed around the excited state and the more electrons have detached, both of which make the second pulse less effective at completing the ionization process. To map out these early-time processes following excitation, we need to directly explore the complementary time dimension to extract the information contained in how the ionization effectiveness of the 2000 nm re-excitation pulse changes with arrival time.

### B. The initial relaxation dynamics following CTTS excitation along the $\tau_2$ time dimension

Figure 3 shows the results of 3-pulse experiments that explore the second time dimension in our atomic ionization reaction. These experiments are different from those shown in Fig. 2 in that the 1250 nm probe pulse is held at a fixed delay time while the arrival time of the 2000 nm re-excitation pulse is scanned relative to the initial 790 nm excitation pulse. Since the 1250 nm probe pulse is fixed at a long delay time, the magnitude of the difference signal along the  $\tau_2 - \tau_1$  time dimension [shown as the circles in Fig. 3(A)] tracks the number of electrons that were relocalized by the 2000 nm re-excitation pulse and did not recombine before being interrogated by the probe pulse. In other words, the difference signal shows how the height of the long-time

relocalization offset in Fig. 2 varies with the arrival time of the 2000 nm pulse. We note that Sension *et al.* have presented a brief report describing a related three-pulse experiment on the  $\text{Na}^-$ -THF system,<sup>20</sup> but they employed a second pulse tuned to 1100 nm that re-excited a combination of solvated electrons and neutral sodium anions [cf. Fig. 1(A)], making interpretation of the resulting difference signals challenging.

Figure 3(A) shows the results when the 1250 nm pulse was placed  $\sim 500$  ps after the initial 790 nm excitation pulse. At this long delay time, all the electrons in immediate and solvent-separated contact pairs will have recombined so that only free electrons created by the re-excitation pulse contribute to the three-pulse difference signal. Thus, the difference signal shown by the circles in Fig. 3(A) represents the fraction of electrons excited by the 790 nm pulse at time zero that were ionized into free electrons by re-excitation at 2000 nm during the first 6 ps. The three-pulse difference signal, however, depends not only on the time-dependent relocalization probability of the electrons re-excited by the 2000 nm pulse but also on the time-dependent population of electrons available to be re-excited at 2000 nm. The solid curve in Fig. 3(A) shows the population of electrons present as a function of time after the initial 790 nm pulse, measured in a separate two-pulse 790 nm pump/2000 nm probe experiment. Since this data tell us the way the electron population changes with time, we can take the ratio of the three-pulse difference and two-pulse signals in Fig. 3(A) to divide out the time-dependent change in population.

To take this ratio and thus combine the information from the two time dimensions, we first subtract off the long-time signal offset resulting from free electrons in the two-pulse experiment, since re-excitation of free electrons does not produce a difference signal at long times.<sup>10</sup> Once this is done, the resulting curve [3P/2P, dashed curve in Fig. 3(B)] provides a direct measurement of the relocalization efficiency (or 1 + 1 ionization probability) of  $\text{Na}^-$  as a function of the arrival time of the 2000 nm pulse. We note that the three-pulse and two-pulse experiments shown in Fig. 3(A) were run back-to-back and that the propagation path of the laser beams was not modified between the two experiments. Thus, we are confident that the position of the zero of time is identical in both experiments, and that both experiments have identical time resolution [as determined by the cross-correlation of the 790 and 2000 nm pulses, which are shown as the dashed curves in Figs. 3(A) and 3(B)].

Figure 3(B) shows that the 3P/2P ratio reaches its maximum value at time zero and then decays to a plateau after  $\sim 1$  ps. The shape of the 3P/2P curve makes sense given that the three-pulse difference signal rises at our instrument limit while the two-pulse electron population signal shows a delayed appearance due to the time needed for solvent relaxation to cause detachment of the excited electron. Perhaps not surprisingly, the highest ionization efficiency of the 2000 nm pulse occurs *prior* to ejection of the electron from excited  $\text{Na}^-$ . This indicates that the 2000 nm re-excitation pulse can complete the 1 + 1 ionization of  $\text{Na}^-$  most effectively only before solvent relaxation stabilizes the initially prepared excited state. In previous work, we noted that if the

2000 nm re-excitation pulse arrived within a few hundred femtoseconds of the 790 nm pump pulse, the effect of the two pulses was additive: The same distribution of free electrons was produced by the 790 nm/2000 nm pulse pair as by a single (560 nm) pulse that had the same total energy.<sup>10</sup> In other words, as long as there has not been significant solvent relaxation, it does not matter when the excess energy needed to ionize (relocalize) the electron arrives. Thus, the 3P/2P curve shown in Fig. 3(B) provides a direct window on the solvent relaxation that follows the initial 790 nm excitation: As time goes on, motions of the solvent create an increasingly deep trap for the excited electron (ultimately trapping the electron by detachment), making it increasingly difficult for the re-excitation pulse to relocalize the excited electron. Moreover, Fig. 3(B) shows that the solvent relaxation and detachment dynamics following the initial 790 nm excitation are not complete until times after  $\sim 1$  ps, when the constant relocalization efficiency indicates that the excited electrons have localized into the deepest possible trap by detachment into immediate contact pairs.

Thus, to the best of our knowledge, Fig. 3 represents the first direct measurement of the initial relaxation processes *during* electron photodetachment from an atom in a liquid. After repeating this experiment multiple times, we have determined that the decay of the relocalization efficiency can be approximately fit to a single exponential with a time constant of  $450 \pm 100$  fs. This is the time over which the electron loses most of its ability to be ionized by the 2000 nm re-excitation pulse.

We can gain even more information from the second time dimension in our three-pulse photoionization experiment by varying the arrival time of the fixed 1250 nm probe pulse. The circles in Fig. 3(C) show the three-pulse difference signal when the 1250 nm probe pulse is fixed to arrive 10 ps after the initial 790 nm excitation. At this early probe arrival time, the three-pulse difference signal not only measures the effect of the 2000 nm re-excitation pulse on free solvated electrons, but also measures the effect on solvated electrons in solvent-separated contact pairs. Figure 3(C) shows that the early-time solvent trapping of the excited electron is similar to that when probing at 500 ps [cf. Figs. 3(A) and 3(B)], indicating that solvent-separated electrons are more efficiently produced by re-excitation of the initial excited state of  $\text{Na}^-$  than by re-excitation of immediate contact-pair electrons. At longer times, however, the three-pulse difference signal in Fig. 3(C) decays to a smaller value than that in Fig. 3(B), and in fact, the difference signal in Fig. 3(C) becomes negative at times longer than  $\sim 4$  ps. This negative difference signal indicates that the 2000 nm pulse *reduces* the amount of 1250 nm absorption by solvated electrons at 10 ps delay. The only way that the 2000 nm re-excitation pulse can reduce the population of electrons is by increasing the rate of recombination of solvent-separated contact pairs. In fact, in previous work we saw that re-excitation of electrons in solvent-separated pairs led to some relocalization into immediate pairs, leading to a net enhancement in recombination at early times after re-excitation.<sup>9,10</sup> Thus, by studying both time dimensions in our three-pulse multiphoton ionization experiment, we cannot only map out

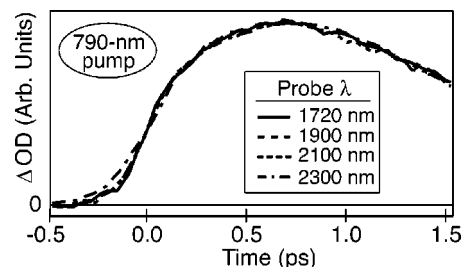


FIG. 4. Two-pulse experiments exciting  $\text{Na}^-$  at 790 nm and probing at a variety of wavelengths in the spectral region where the detached solvated electron absorbs [cf. Fig. 1(A)]. The wavelength-independent decay kinetics suggests that there is little solvent relaxation after electron detachment is complete. Note that the solvent is responsible for the slight broadening of the 2300 nm signal, as the onset of the THF absorption in the mid-IR produces a large group velocity mismatch between the 790 nm pump and 2300 nm probe beams.

the solvent relaxation around the initially prepared excited state, but we can also determine the fate of the electrons re-excited from different locations in the solvent.

#### IV. DISCUSSION

All of the data in Fig. 3 make it clear that the  $\sim 450$  fs time constant represents a solvent relaxation process that dynamically prevents the relocalization of the excited electron. In a series of mixed quantum/classical molecular dynamics simulations of the  $\text{Na}^-$  ionization,<sup>16</sup> we have shown that the 450 fs relaxation corresponds to the time it takes the solvent to stabilize the CTTS-excited electron. Upon 790 nm excitation, the valence  $\text{Na}^- 3s$  electron is converted into a  $p$ -like excited state supported by the spherical solvent cavity surrounding the anion. The simulations suggest that the new  $p$ -like charge distribution is best stabilized by placing the positive end of the solvent dipoles between the two lobes of the excited negative charge. When the solvent dipoles try to enter the node in the excited-state wave function, however, they are blocked by the presence of the sodium atom lying at the center of the charge distribution. Thus, to promote relaxation, the solvent works to move the node off the sodium atom, leaving one lobe pinned to the atom and the other extended out into the solvent.<sup>16</sup> We believe that the data in Fig. 3(B) provide a direct measure of this *nodal migration*, which takes  $\sim 450$  fs to complete, and therefore, occurs before electron detachment.

As we pointed out earlier, however, Ruhman and co-workers believe that electron detachment following the CTTS excitation of  $\text{Na}^-$  is an ultrafast ( $< 200$  fs) process; in their picture, the bulk of the solvent relaxation occurs after detachment and only serves to stabilize the ground state of the detached solvated electron.<sup>11</sup> To distinguish whether or not our observed  $\sim 450$  fs solvent relaxation occurs before or after detachment, we have performed a series of separate experiments monitoring the formation of the detached electron as a function of probe wavelength. Figure 4 shows that the appearance dynamics of the solvated electron's absorption are independent of wavelength, indicating that the entire absorption band rises and decays uniformly. Thus, the absorption kinetics measured in the  $\sim 2 \mu\text{m}$  spectral region

reflect changes in the population of detached solvated electrons: The lack of probe wavelength dependence verifies that there is no significant solvent relaxation after detachment is complete. Overall, the results in Fig. 4 support the idea of a photodetachment process induced by solvent motions that cause nodal migration of the excited state of the sodide anion; a process that occurs on a time scale slower than our  $\sim 200$  fs time resolution.

In addition to explaining the three-pulse experiments shown in Fig. 3, we believe that pre-detachment solvent relaxation is also the process that produces the fast initial decay seen in the two-pulse 790 nm pump–1250 nm probe signal presented in Fig. 2(A). It makes sense that the 1250 nm absorption of the excited electron would change during the process of nodal migration.<sup>16</sup> However, it is virtually impossible to extract any quantitative information about this early-time relaxation from the data in Fig. 2(A) because the 1250 nm signal also includes contributions from solvated neutral sodium atoms and detached solvated electrons, which have different absorption cross-sections [cf. Fig. 1(A)]. The fact that the early time relaxation is directly manifest in the data in Fig. 3 serves to highlight the power of multi-pulse electronic spectroscopy. Since the multi-pulse experiment works selectively by re-exciting only a single chemical intermediate, it provides a means to remove interference from other species and extract information about solvent relaxation processes that are not directly available in conventional two-pulse experiments.

Together, the data in Figs. 2–4 have helped us to build a molecular-level picture of the early-time dynamics underlying the photodetachment of electrons from atomic ions in liquids. For  $\text{Na}^-$  in THF, the initial solvent relaxation accompanying excitation takes  $\sim 450$  fs to complete, and likely involves migration of the angular node of the excited state wave function off the Na atom.<sup>16</sup> Once nodal migration is complete, detachment can then take place because a significant fraction of the electronic charge density is extended out into the solvent. This implies that the time for detachment of the excited electron must be slower than the initial  $\sim 450$  fs solvent relaxation, an idea which stands in contrast to other reports that detachment takes place in  $< 200$  fs in this system,<sup>11</sup> but which fits well with the  $\sim 700$  fs detachment time that we have determined in previous work.<sup>7</sup>

In summary, we have demonstrated the application of multi-pulse electronic population spectroscopy to study the photoionization of atomic ions in liquids. For the sodide CTTS reaction, the important relaxation processes that take place following the initial excitation occur in  $\sim 450$  fs, the time it takes molecules of the liquid to rearrange and trap the excited electron. However, even with sophisticated three-pulse experiments, it is difficult to distinguish between sol-

vent relaxation around an excited electron trapped in a solvent cavity with an atom and an ionized or detached solvated electron. Clearly, further effort is needed to unravel the early time dynamics and to build a molecular picture of how atomic photodetachment proceeds in solution. The 1+1 resonant two-photon ionization experiments that we have presented have explored only the dynamics along the axes of the two time dimensions available with three laser pulses. Our hope is that incorporation of a third dimension by changing the wavelength of the re-excitation pulse will shed new light on the nature of electron photodetachment from atoms in liquids.

## ACKNOWLEDGMENTS

This work was supported by NSF Grant No. CHE-0204776; B.J.S. is a Camille Dreyfus Teacher-Scholar and a Cottrell Scholar of Research Corp.

- <sup>1</sup>P. F. Tian, D. Keusters, Y. Suzuki, and W. S. Warren, *Science* **300**, 1553 (2003).
- <sup>2</sup>J. D. Hybl, A. A. Ferro, and D. M. Jonas, *J. Chem. Phys.* **115**, 6606 (2001).
- <sup>3</sup>N. Demirdoven, M. Khalil, and A. Tokmakoff, *Phys. Rev. Lett.* **89**, 7401 (2002).
- <sup>4</sup>L. J. Kaufman *et al.*, *Phys. Rev. Lett.* **88**, 7402 (2002).
- <sup>5</sup>M. P. Debreczeny, W. A. Svec, E. M. Marsh, and M. R. Wasielewski, *J. Am. Chem. Soc.* **118**, 8174 (1996); A. S. Lukas, P. J. Bushnard, and M. R. Wasielewski, *ibid.* **123**, 2440 (2001).
- <sup>6</sup>D. H. Son, P. Kambhampati, T. W. Kee, and P. F. Barbara, *Chem. Phys. Lett.* **342**, 571 (2001); T. W. Kee, D. H. Son, P. Kambhampati, P. F. Barbara, *J. Phys. Chem. A* **105**, 8434 (2001); D. H. Son, P. Kambhampati, T. W. Kee, and P. F. Barbara, *ibid.* **105**, 8269 (2001).
- <sup>7</sup>E. B. Barthel, I. B. Martini, and B. J. Schwartz, *J. Phys. Chem. B* **105**, 12330 (2001); E. R. Barthel, I. B. Martini, E. Keszei, and B. J. Schwartz, *J. Chem. Phys.* **118**, 5916 (2003).
- <sup>8</sup>E. R. Barthel and B. J. Schwartz, *Chem. Phys. Lett.* **375**, 435 (2003).
- <sup>9</sup>I. B. Martini, E. B. Barthel, and B. J. Schwartz, *Science* **293**, 462 (2001).
- <sup>10</sup>I. B. Martini, E. B. Barthel, and B. J. Schwartz, *J. Am. Chem. Soc.* **124**, 7622 (2002).
- <sup>11</sup>Z. Wang, O. Shoshan, B. Hou, and S. Ruhman, *J. Phys. Chem. A* **107**, 3009 (2003).
- <sup>12</sup>W.-S. Sheu and P. J. Rossky, *J. Chem. Phys.* **103**, 2642 (1996).
- <sup>13</sup>M. J. Blandamer and M. F. Fox, *Chem. Rev. (Washington, D.C.)* **70**, 59 (1970).
- <sup>14</sup>S. E. Bradforth and P. Jungwirth, *J. Phys. Chem. A* **106**, 1286 (2002); V. H. Vilchiz, J. A. Kloepfer, A. C. Germaine, V. A. Lenchenkov, and S. E. Bradforth, *ibid.* **105**, 1711 (2001); V. A. Lenchenkov, J. A. Kloepfer, V. H. Vilchiz, and S. E. Bradforth, *Chem. Phys. Lett.* **342**, 277 (2001).
- <sup>15</sup>J. Peon, G. C. Hess, J.-M. L. Pecourt, T. Yuzawa, and B. Kohler, *J. Phys. Chem. A* **103**, 2460 (1999).
- <sup>16</sup>C. J. Smallwood, W. B. Bosma, R. E. Larsen, and B. J. Schwartz, *J. Chem. Phys.* **119**, 11263 (2003).
- <sup>17</sup>J. L. Dye, *J. Phys. Chem.* **84**, 237 (1980).
- <sup>18</sup>I. B. Martini, E. R. Barthel, and B. J. Schwartz, *J. Chem. Phys.* **113**, 11245 (2000).
- <sup>19</sup>T.-Q. Nguyen, I. B. Martini, J. Liu, and B. J. Schwartz, *J. Phys. Chem. B* **104**, 237 (2000).
- <sup>20</sup>R. J. Sension, Z. Wang, O. Shoshana, B. Hou and S. Ruhman, *Proc. 12th Int. Conf. Ultrafast Phenom.; Springer Ser. Chem. Phys.* **71**, 462 (2003).